PNAS RESEARCH ARTICLE | MICROBIOLOGY

A commensal-encoded genotoxin drives restriction of *Vibrio cholerae* colonization and host gut microbiome remodeling

Jiandong Chen[a,1], Hyuntae Byun[a,1], Rui Liu[b,1], I-Ji Jung[a,1], Qinqin Pu[a], Clara Y. Zhu[c], Ethan Tanchoco[b], Salma Alavi[b], Patrick H. Degnan[b], Amy T. Ma[d], Manuela Roggiani[e], Joris Beld[d], Mark Goulian[e], Ansel Hsiao[b,2], and Jun Zhu[a,2]

Edited by Dennis Kasper, Harvard Medical School, Boston, MA; received November 21, 2021; accepted February 1, 2022

Members of complex microbial communities that reside in environments such as the mammalian gut have evolved mechanisms of interspecies competition, which may be directed at resident microbial and host cells. While previous work has focused mainly on metabolic or niche competition, few specific intermicrobial targeting mechanisms have been elucidated in the mammalian gut. Here, we show that a genotoxin produced by commensal *Escherichia coli*, colibactin, which was previously shown to induce DNA damage in host intestinal cells, is also able to target via a contact-dependent mechanism a variety of enteric pathogens and commensals, including the important human diarrheal pathogen *Vibrio cholerae*. We find that colibactin-mediated killing depends on accumulation of intracellular reactive oxygen species, leading to DNA damage and loss of target cell fitness. We also show that the presence of colibactin is associated with cholera outcomes in a large human metagenomic dataset and that colibactin can shape the microbiome by species-specific targeting of a common human gut-associated microbe *Bacteroides fragilis*, suggesting that genotoxin-mediated mechanisms may have broad effects in the complex polymicrobial interactions that shape commensal microbial communities and their effects on host health and disease.

colibactin | *Vibrio cholerae* | microbiome

Significance

In a polymicrobial battlefield where different species compete for nutrients and colonization niches, antimicrobial compounds are the sword and shield of commensal microbes in competition with invading pathogens and each other. The identification of an *Escherichia coli*–produced genotoxin, colibactin, and its specific targeted killing of enteric pathogens and commensals, including *Vibrio cholerae* and *Bacteroides fragilis*, sheds light on our understanding of intermicrobial interactions in the mammalian gut. Our findings elucidate the mechanisms through which genotoxins shape microbial communities and provide a platform for probing the larger role of enteric multibacterial interactions regarding infection and disease outcomes.

The human gut hosts a complex gastrointestinal ecosystem, consisting of a diverse array of commensal microbial populations. One role of this ecosystem is safeguarding gut health by defending against invading pathogens (1). This protection, known as colonization resistance, has been long documented in rodents (2) and can be achieved via diverse mechanisms, including nutrient competition, niche occupation, immunomodulation, and production of antimicrobial toxins (3–6). Recent studies of gut microbiota illustrate that bacterial antagonism is pervasive and that, in addition to warding off pathogens, it also affects the overall structure, dynamics, and composition of host-associated microbial communities (3, 7).

Vibrio cholerae is an enteropathogen that infects the human small intestine and causes the severe acute diarrheal disease cholera by using cholera toxin and toxin-coregulated pilus as the primary factors for virulence and colonization, respectively (8). Over the years, several engineered or natural commensals directly targeting virulence factors or virulence signaling have been reported that enable colonization resistance toward or clearance of *V. cholerae* infection in animal models (6, 9–11). In other cases, commensals known to produce acidic metabolites also effectively protect hosts from *V. cholerae* infection (12–14). While the role of human-associated microbes has been characterized in some detail (5, 6), the level of colonization resistance is not as profound as that observed in mice. The high resistance of the mouse gut microbiota to *V. cholerae* infection (2) thus offers the possibility of identifying insights into mechanisms of microbiome-mediated colonization resistance.

In this study, we began by identifying enteric commensals in the mouse intestine with deleterious effects upon *V. cholerae* infection. Through screening more than 100 lactose-fermenting enteric bacterial isolates from both the small and large intestines of adult mice, we found a handful of strains that could potently inhibit *V. cholerae* growth. In-depth analysis of one isolate, a B2 phylogroup *Escherichia coli* harboring a polyketide synthase (*pks*) island, demonstrated that the genotoxin colibactin encoded by the *pks* island is essential for antagonizing *V. cholerae* in vitro and during mouse colonization. Produced by commensal and pathogenic enterobacteria, colibactin is a natural genotoxin that damages double-stranded DNA via DNA cross-linking (15, 16). It is closely linked to tumorigenic effects in colorectal cancer (17), but its effects on other microbes or the gut microbiota are largely unknown. Here, we determine the DNA-damaging effects of *pks E. coli* on *V. cholerae* and explore their ecological effects on the gut microbiota.

Author contributions: J.C., H.B., R.L., I.-J.J., Q.P., M.G., A.H., and J.Z. designed research; J.C., H.B., R.L., I.-J.J., Q.P., C.Y.Z., E.T., S.A., A.T.M., M.R., and J.B. performed research; P.H.D. contributed new reagents/analytic tools; J.C., H.B., R.L., I.-J.J., Q.P., C.Y.Z., E.T., S.A., P.H.D., A.T.M., J.B., A.H., and J.Z. analyzed data; and J.C., H.B., R.L., I.-J.J., P.H.D., A.T.M., J.B., M.G., A.H., and J.Z. wrote the paper.

The authors declare no competing interest.

This article is a PNAS Direct Submission.

[1]J.C., H.B., R.L., and I.-J.J. contributed equally to this work.

[2]To whom correspondence may be addressed. Email: ansel.hsiao@ucr.edu or junzhu@pennmedicine.upenn.edu.

This article contains supporting information online at http://www.pnas.org/lookup/suppl/doi:10.1073/pnas.2121180119/-/DCSupplemental.

Published March 7, 2022.

Results

Contact-Dependent Killing of *Vibrio* by an *E. coli* Isolate from the Mouse Intestines. To investigate how commensal bacteria in the gastrointestinal tract affect *V. cholerae* growth, we spread the intestinal contents of 10 CD-1 mice on MacConkey agar plates and selected over 140 pink colonies representing lactose-fermenting enterobacteria, such as *E. coli* and *Klebsiella*. These colonies were grown in Luria–Bertani (LB) medium overnight and mixed with *V. cholerae* C6706 (referred as *Vc* hereafter) in 96-well plates containing M9 minimal medium. The plates were incubated at 37 °C for 24 h without shaking (mimicking the microaerobic condition that *Vc* may encounter during colonization of the small intestine), and the cultures were diluted and spotted on selective LB polymyxin B agar plates that only permit *Vc* growth. We identified nine isolates that significantly inhibited *Vc* growth (Fig. 1*A*). We then performed quantitative liquid assays and confirmed that these strains inhibited *Vc* growth, effectively reducing *Vc* populations from three to five orders of magnitude compared to *Vc* monoculture (Fig. 1*B*). Then, 16S rRNA sequencing indicated that all nine highly *Vc*-inhibiting strains were *E. coli*. As controls, coculture of either *E. coli* K12 strain MG1655 or MP1, a mouse commensal previously isolated from CD-1 fecal samples (18), had no effect on *Vc* growth (Fig. 1*B*). We selected F10, which was isolated from the small intestine, for further studies, as it was susceptible to P1 transduction with higher efficiency (*SI Appendix*, Fig. S1), which facilitated downstream genetic manipulation. We named this *E. coli* strain *E. coli* mouse small intestine isolate 1 (EMS1). Genome sequencing of EMS1 (19) revealed it to be a member of the phylogenetic group B2. Whole-genome alignment of EMS1 with other *E. coli* strains showed homology with human uropathogenic *E. coli* CFT073 and 536 as well as with the probiotic human fecal isolate Nissle 1917 (*SI Appendix*, Fig. S2*A*). Average nucleotide identity (ANI) analysis of EMS1 with representatives of phylogenetic groups A, B1, B2, D, E, and S showed clustering of EMS1 with B2 strains with >98% ANI (*SI Appendix*, Fig. S2*B*).

EMS1 Kills *V. cholerae* In Vitro. We then more closely examined the effects of EMS1 on *Vc* growth. Coculture of *Vc* and EMS1 at different ratios displayed an EMS1 dose-dependent inhibition of *Vc* growth (Fig. 1*C*). Importantly, in the presence of EMS1, *Vc* populations grew to mid-log phase before crashing (Fig. 1*D*), suggesting that EMS1 effectively kills *Vc*. *Vc* is sensitive to low pH, but the killing effect from EMS1 was not due to growth medium acidification, as the pH was similar between cultures with and without EMS1 cocultivation (*SI Appendix*, Fig. S3). When we separated *Vc* and EMS1 using dialysis membranes with a 10-kDa molecular weight cutoff, EMS1 no longer exhibited bactericidal effects toward *Vc* (Fig. 1*E*), suggesting that the killing effect is likely contact dependent. An alternative explanation is that the membrane may prevent the active compounds produced by EMS1 from reaching *Vc*.

V. cholerae has over 200 known serotypes, but only strains with O1 and O139 antigens are known to cause epidemic disease (20). The O1 serogroup is further divided into O1 Classical and El Tor biotypes on the basis of other physiological properties. We examined whether EMS1 affected the growth of different *V. cholerae* strains. We mixed EMS1 with various *V. cholerae* strains (*SI Appendix*, Table S1) and found that EMS1 exhibited a killing effect toward all *V. cholerae* strains tested (Fig. 1*F*). Moreover, EMS1 also inhibited the growth of other *Vibrio* species, such as *V. fischeri*, *V. fluvialis*, and *V. harveyi*. These data suggest that EMS1 has a broad spectrum of anti-*Vibrio* activity.

EMS1-Produced Colibactins Are Responsible for the Anti-*Vibrio* Activity. To investigate the molecular mechanism responsible for EMS1 killing of *Vc*, we performed a genetic screen by transposon mutagenizing EMS1 and screening for mutants that lost the anti-*Vibrio* activity (Fig. 2*A*). From ∼3,000 Tn5 mutants, we obtained 3 candidates in which anti-*Vibrio* activity was abolished (Fig. 2*B*). Sequencing analysis showed that these mutants all had transposons inserted in different loci of the *pks* genomic island (Fig. 2*C*, triangles represent transposon insertion), encoding a putative hybrid nonribosomal peptide synthetase–polyketide synthase assembly line that is responsible for synthesis of colibactin (21). Alignment of the biosynthetic gene cluster (BGC) for colibactin shows that EMS1 harbors a colibactin BGC analogous to those of Nissle 1917, CFT073, and 536 (*SI Appendix*, Fig. S2*A*). To confirm the involvement of colibactin synthesis in EMS1's anti-*Vibrio* activity, we constructed in-frame deletion mutants in *clbN*, encoding a synthase involved in the initiation of colibactin biosynthesis (22), and in *clbL*, encoding an amidase that is required for colibactin maturation (23). Deletions in either *clbN* or *clbL* in EMS1 completely abolished the vibriocidal effect (Fig. 2*D*). Complementation of *clbN* or *clbL* in *trans* restored the observed killing. These data suggest that the anti-*Vibrio* activity of EMS1 is contingent upon colibactin synthesis.

The colibactin BGC produces several intermediates that can be detected in crude cellular extracts of *E. coli* source strains. Liquid chromatography–mass spectrometry (LC–MS) analysis of a crude extract of EMS1 showed the presence of C14-D-Asn, an abundant diagnostic metabolite of the colibactin BGC (Fig. 2*E*). C14-D-Asn is both the hydrolysis product of an intermediate synthesized on ClbN as well as the ClbP-catalyzed cleavage product of precolibactin-1492 (24). Deletion of *clbN* abolishes production of C14-D-Asn, and deletion of the late-stage *clbL* gene retains production, as was previously observed using a plasmid-based colibactin BGC (25). We also observed several other characteristic colibactin BGC metabolites characterized previously (22, 26–28). It should be noted that proteins encoded in the colibactin BGC are involved in the biosynthesis of other metabolites that are potentially bioactive (29, 30). However, both *clbN* and *clbL* mutants were deficient for killing *Vibrio*, suggesting that EMS1 produces classical colibactin that directly antagonizes *Vibrio*. We could detect both left and right ends of *pks* genomic islands in the other eight *E. coli* isolates (Fig. 1) that inhibited *Vc* growth (*SI Appendix*, Fig. S4), implying that these strains likely utilize the same inhibitory mechanisms as that of EMS1.

EMS1-Produced Colibactin Inhibits *V. cholerae* Colonization of the Small Intestine. Next, we used a streptomycin-treated adult mouse model to test whether EMS1 impacts *Vc* colonization in vivo. One day before *Vc* infection, we preinoculated mice with either a blank control or overnight cultures of either EMS1 or Δ*clbN* mutant. We examined *Vc* colonization of the small intestine 5 d postinfection. We found that compared to the blank inoculation, *Vc* colonization was reduced nearly 100-fold in the mice preinoculated with EMS1, whereas precolonization with Δ*clbN* mutants did not affect *Vc* colonization (Fig. 3*A*). However, this result was not due to differential colonization of EMS1 itself, since both the wild-type EMS1 and the Δ*clbN* mutant colonized equally well in the mouse small intestine (Fig. 3*B*). These data suggest that EMS1 inhibits *Vc* colonization in vivo and that the inhibition is dependent on the production of colibactin.

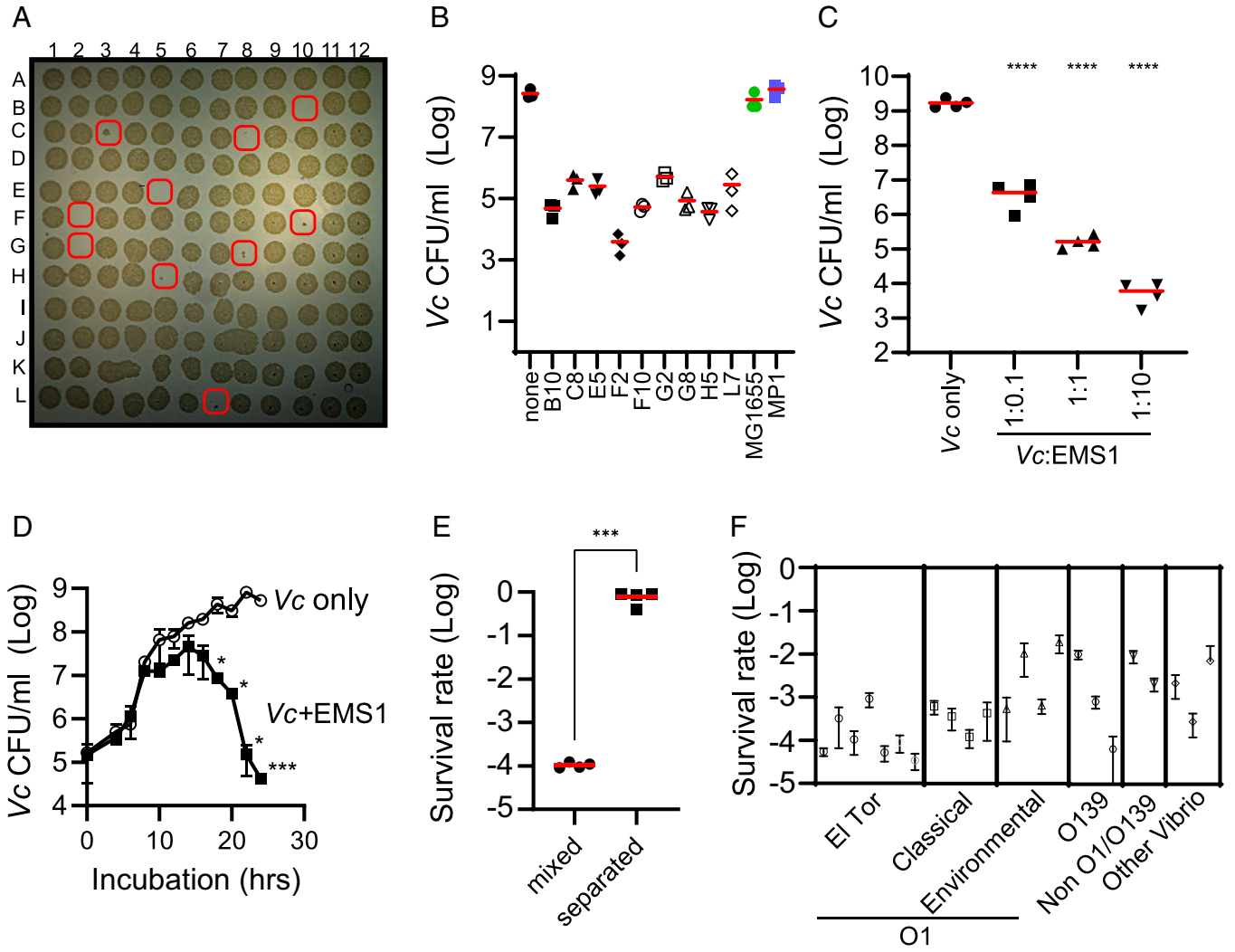

Fig. 1. Anti-*Vibrio* activities exhibited by gut commensal *E. coli*. (*A*) Screening. Mouse-isolated *E. coli* strains were grown to saturation in 96-well plates and then inoculated into minimal medium containing *V. cholerae*. The cultures were incubated at standing 37 °C for 24 h, and viable *V. cholerae* was determined by plating a four-log dilution of the mixed culture on selective LB agar. (*B*) Confirmation of selected mouse *E. coli* isolates on *V. cholerae* growth. *E. coli* isolates identified by the screen and controls (MG1655 and MP1) were coincubated with *V. cholerae* at a 10:1 ratio in minimal medium and incubated at standing 37 °C for 24 h. *V. cholerae* CFU values were determined by serial dilution and plating on selective LB agar plates. The mean of three independent assays is shown. (*C* and *D*) EMS1 kills *V. cholerae* in a dose-dependent manner. *V. cholerae* alone or *V. cholerae* with different ratios of EMS1 was inoculated into M9 medium and incubated without shaking at 37 °C for 24 h. *V. cholerae* CFU values were then determined. The mean of three independent assays is shown, and error bars represent the SD. *$P < 0.05$; ***$P < 0.001$; ****$P < 0.0001$ (one-way ANOVA). (*E*) Contact-dependent killing. EMS1 and *V. cholerae* were separately inoculated into 10-kDa–cutoff dialysis bags in minimal medium or coinoculated into the medium and incubated for 24 h before *V. cholerae* CFU determination. The survival rate was calculated by normalizing CFU of *V. cholerae* cocultured with EMS1 against that of *V. cholerae* cultured alone. The mean of four independent assays is shown; ***$P < 0.001$ (*t* test). (*F*) EMS1 inhibitory effects on various *Vibrio* strains. Overnight cultures (10^6 CFU/mL) of *Vibrio* strains were inoculated into M9 medium without and with 10^7 CFU/mL EMS1 and incubated for 24 h. CFU of *Vibrio* were then determined. The mean of three independent assays is shown, and error bars represent the SD.

The Presence of Colibactin in the Gut Microbiome Is Associated with Less Severe Outcomes of *V. cholerae* Exposure in Human Populations. To examine whether genes involved in colibactin production are associated with divergent cholera outcomes in human populations, we performed an analysis of a shotgun metagenomic deep-sequencing study (Dataset S1) examining the fecal metagenome of a prospective human cholera exposure cohort. Household contacts were enrolled within 6 h of presentation of the index household cholera case and tracked for infection status. Individuals who developed diarrhea were categorized as exposed and symptomatic ("SYM"), and those without diarrhea but whose culture and/or serum tested positive were considered exposed and asymptomatic ("ASYM"). The rest were classified as uninfected ("UNI"). Our analysis of the published shotgun metagenomics sequencing of fecal specimens from these cohorts showed that the relative abundance of reads mapping to the *clb* biosynthetic cluster differed based on exposure outcome; *clb* reads were significantly lower in the fecal microbiomes of SYM contacts than in both ASYM and UNI (Fig. 3*C*). These results thus suggest that the presence of colibactin in the gut microbiome may be associated with different outcomes to *V. cholerae* exposure in humans.

Colibactin Produced by EMS1 Induces DNA Damage in Mammalian Cells and Waxworm Larvae. A signature property of colibactin is the induction of DNA double-strand breaks (DSBs) in mammalian cells (16). To confirm that EMS1 also produces colibactin with this feature, we first monitored the phosphorylation of histone H2AX (γH2AX), a sensitive marker of DSBs (21), in HeLa cells infected with EMS1 or Δ*clbN* mutants for 4 h. We found that EMS1, but not Δ*clbN* mutants, induced γH2AX foci (green) on mitotic chromosomes (stained by pH3-red)

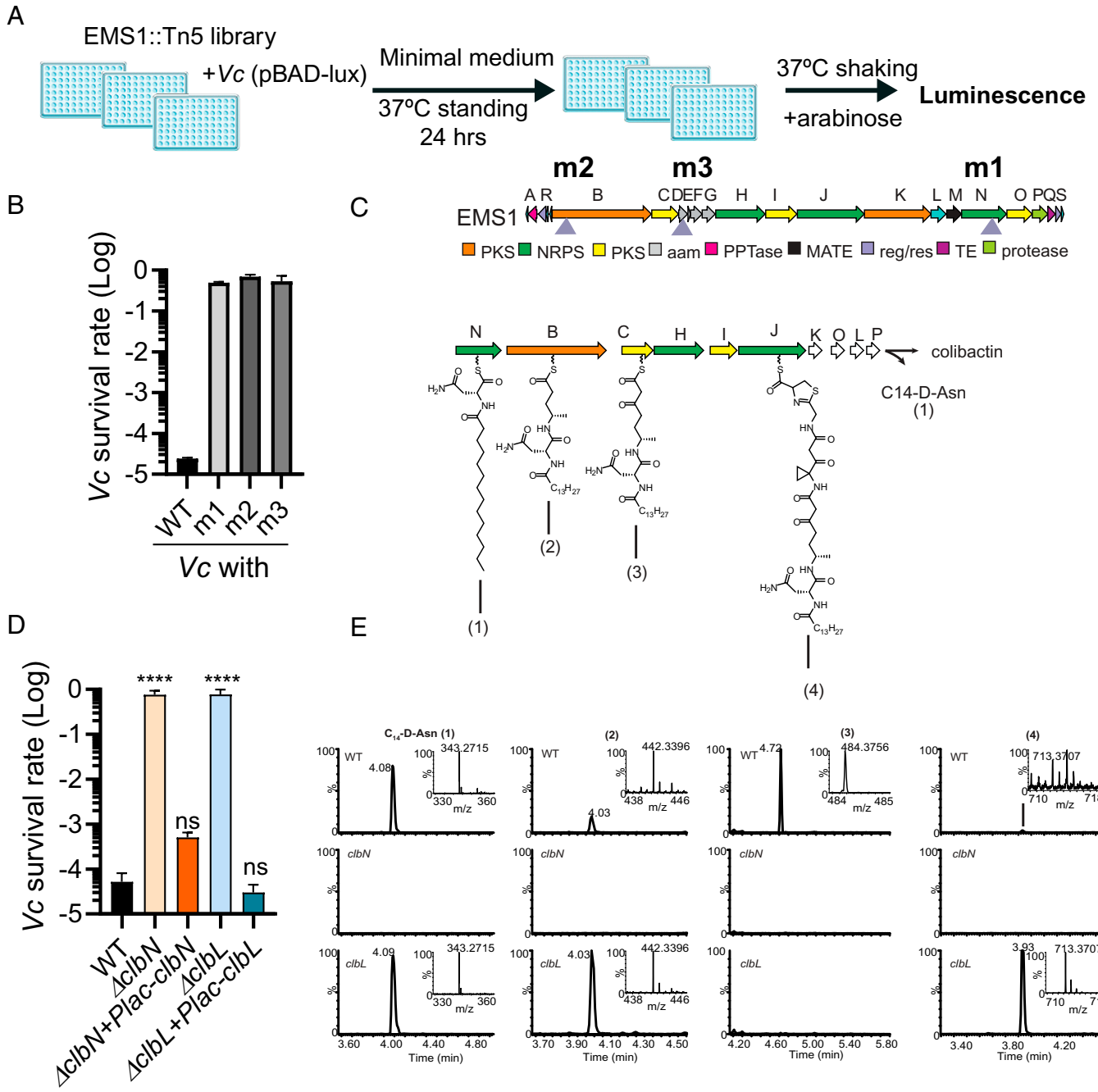

Fig. 2. EMS1 produces colibactin that inhibits *V. cholerae* growth. (*A*) Screening scheme for EMS1 genes responsible for anti-*Vibrio* activity. (*B*) Effects of coculturing transposon mutants of EMS1 on *V. cholerae* growth. *V. cholerae* alone or *V. cholerae* with different EMS1 mutants were inoculated into M9 medium and incubated standing at 37 °C for 24 h. *V. cholerae* CFU were then determined. (*C*) BGC of colibactin. The EMS1 colibactin BGC was extracted and plotted using Easyfig (65). Commonly observed colibactin intermediates (or hydrolysis byproducts) (1 to 4) are drawn as products of *clbN*, *clbB*, *clbC*, and *clbJ*. Triangles represent transposon insertions from the screen performed in *A*. (*D*) The importance of EMS1 *clb* genes in killing *V. cholerae*. *V. cholerae* was cultured alone or cocultured with EMS1 *clb* mutants and their complements for 24 h; ****$P < 0.0001$ (one-way ANOVA). ns, no significance. (*E*) Colibactin metabolites from wild-type (WT), Δ*clbN*, and Δ*clbL* strains of EMS1. Culture extracts were analyzed by LC–MS for the presence of colibactin intermediates 1 to 4 (as shown in *C*), and extracted ion chromatograms and mass spectra (*Insets*) are shown. NRPS, nonribosomal peptide synthetase; AAM, genes involved in biosynthesis of 1-aminocyclopropanecarboxylic acid moiety; PPTase, 4′-phosphopantetheinyl transferase; MATE, multidrug and toxic compound extrusion transporter; Reg/res, genes involved in regulation and resistance; TE, thioesterase.

(31), suggesting that EMS1 produces colibactin that can induce DNA damage in mammalian cells in vitro (*SI Appendix*, Fig. S5*A*).

We used larvae of the wax moth *Galleria mellonella* as a model to examine whether EMS1 induces DNA damage in vivo. We injected 10 μL (10^4 colony-forming units [CFU]) of either EMS1 wild type or Δ*clbN* mutant into the larvae. Only 25% of larvae were alive at 48 h after infection for wild type, whereas more than 75% of larvae survived Δ*clbN* injection, indicative of colibactin-induced lethality in wax moth larvae (*SI Appendix*, Fig. S5*B*). We quantified plasma phenoloxidase (PO) activity, a proxy for immune response, in EMS1-infected insects. We found that PO levels in larvae infected with wild-type EMS1 were significantly higher than in Δ*clbN*-treated insects (*SI Appendix*, Fig. S5*C*). Similarly, the levels of antimicrobials in the hemolymph of larvae infected with EMS1

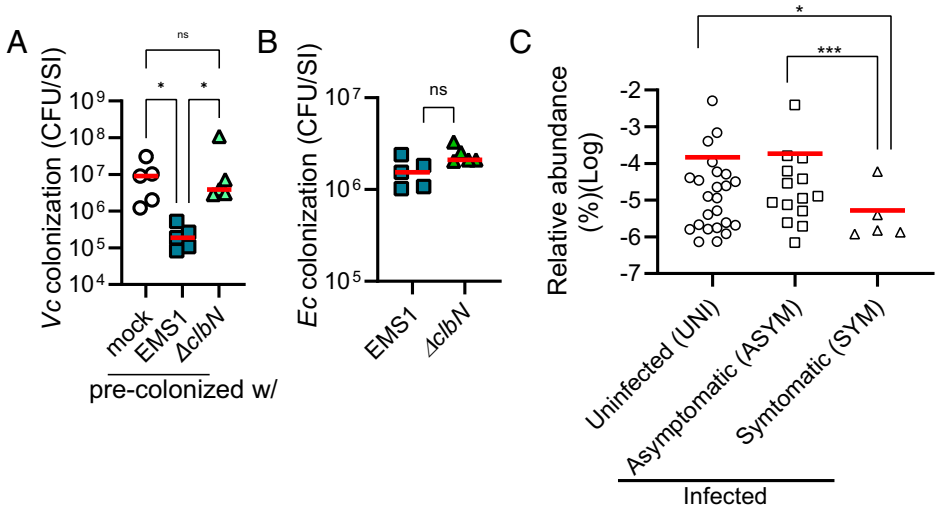

Fig. 3. Colibactin affects *V. cholerae* colonization, and colibactin biosynthetic genes are negatively correlated to cholera symptoms in human populations. (*A* and *B*) Six-week-old CD-1 mice were treated with streptomycin and colonized without or with either EMS1 or Δ*clbN E. coli*. Wild-type *V. cholerae* was then inoculated after 1 d. After 5 d, small intestines were retrieved, and CFU values of colonized *V. cholerae* (*A*) and *E. coli* (*Ec*) (*B*) were enumerated. Horizontal lines represent the average number of colonized bacteria from 5 mice. $*P < 0.05$ (two-way ANOVA). ns, no significance. SI, small intestine. w/, with. (*C*) Log relative abundance values of *pks* genes in human shotgun fecal microbiomes of cholera patients (62) or their household contacts that remained uninfected or asymptomatically colonized are shown. Of all the samples, *pks* genes were not detected in 21 of 45 UNI, 10 of 24 ASYM, and 8 of 13 SYM individuals; edgeR: $*P < 0.05$; $***P < 0.001$.

were higher than those found in Δ*clbN*-infected larvae (*SI Appendix*, Fig. S5*D*), suggesting that colibactin triggers the production of antimicrobial factors. To examine whether EMS1 infection induces DNA damage in larvae, we performed comet assays (32) to detect DNA lesions in larval hemolymph cells exposed to EMS1 or Δ*clbN* for 48 h. The comet tail moment increased in EMS1-infected cells compared with the phosphate-buffered saline and Δ*clbN* controls (*SI Appendix*, Fig. S5 *E* and *F*), indicating that colibactin produced by EMS1 induces DNA damage in vivo.

Colibactin Induces *V. cholerae*'s SOS Response and Reactive Oxygen Species Accumulation under Microaerobic Conditions. Next, we investigated how EMS1-produced colibactin serves as an antibiotic against *V. cholerae*. We first examined whether oxygen levels affect colibactin function. Compared to microaerobic conditions, EMS1 grown under aerobic conditions was incapable of killing *Vc* (Fig. 4*A*). *clbB* is the first gene of the *clb* operon. We measured the expression of a *clbB–lacZ* transcriptional fusion and found that *clbB* was more highly expressed under oxygen-limiting conditions (Fig. 4*B*), consistent with the observation that more effective killing occurred under static microaerobic conditions, which *V. cholerae* encounters during infection.

Colibactin induces DSBs in eukaryotic cells (*SI Appendix*, Fig. S5 and ref. 16). We examined whether EMS1-produced colibactin might similarly induce DNA damage in *V. cholerae* cells. We constructed a chromosomal *recA–gfp* transcriptional fusion in *Vc* to monitor DNA damage. DNA-damaging agents such as fluoroquinolones activate the SOS response pathway, including *recA* (33); as expected, sublethal doses of ciprofloxacin strongly activated *recA* expression in *Vc* (*SI Appendix*, Fig. S6). Compared to *Vc* alone, cocultivation with EMS1, but not with Δ*clbN*, significantly induced *recA–gfp* expression in *Vc* cells (Fig. 4*C*). These results suggest that colibactin produced by EMS1 may cause DNA damage in *Vc* cells. We also measured intracellular reactive oxygen species (ROS) accumulation using the redox-sensitive, cell-permeable dye 2′,7′-dichlorodihydrofluorescein diacetate (DCFDA). Compared to monocultured *Vc*, the presence of wild-type EMS1, but not of Δ*clbN*, resulted in significantly more accumulated ROS in *Vc* (Fig. 4*D*). Although it is disputed whether ROS production is a common effect of antibiotics that cause antimicrobial killing (34–36), we speculate that elevated ROS levels due to EMS1-produced colibactin are likely detrimental to *Vc* survival.

Colibactin-Dependent Growth Inhibition toward Other Bacterial Species. To test whether EMS1 inhibits the growth of bacteria other than *Vibrio* in a *clb*-dependent manner, we cocultured either wild-type EMS1 or Δ*clbN* mutants with a panel of mostly pathogenic bacteria (Fig. 5*A* and *SI Appendix*, Table S2). We found that EMS1 did not affect the growth of other *E. coli* strains tested nor did it affect *Acinetobacter*, *Pseudomonas*, *Bacillus*, *Enterococcus*, or *Streptococcus*. However, EMS1 inhibited growth of one *Enterobacter aerogenes* strain and three *Staphylococcus* strains tested (Fig. 5*A*). It also mildly affected two *Clostridium difficile* strains. In one previous study (37), it has been shown that pks^+ *E. coli* elicits antibiotic activity against a number of *Staphylococcus aureus* clinical isolates, but the killing efficiency is relatively low (~fourfold). Here, EMS1 inhibited *S. aureus* growth by one to three orders of magnitude. This could be due to the potency of colibactin production by EMS1 or differences in tested culturing conditions.

To better understand why EMS1 can kill some bacteria but not others, we conducted a genomic library screen (Fig. 5*B*). We first constructed a plasmid-based genomic library of *E. coli* MG1655, which is resistant to EMS1 (Fig. 5*A*), and introduced the library into *Vc*. The resulting *Vc* transconjugants were screened for resistance to EMS1. From ~5,000 clones, we identified 1 *Vc* isolate harboring a ~6-kilobase MG1655 fragment (Fig. 5*C*) that increased *Vc* EMS1 survival rate by 100-fold over the vector control (Fig. 5*D*). Sequencing of the *E. coli* fragment revealed it to contain the *recG* gene, encoding a DNA helicase in *E. coli* that plays a role in DNA DSB repair. Overexpressing this *E. coli recG* in *Vc* effectively prevented EMS1 killing (Fig. 5*D*) and reduced EMS1-mediated ROS accumulation (Fig. 5*E*). These results reinforce the idea that the mechanism of colibactin killing of *Vc* is through induction of DNA damage and that the bacteria resistant to EMS1 killing may

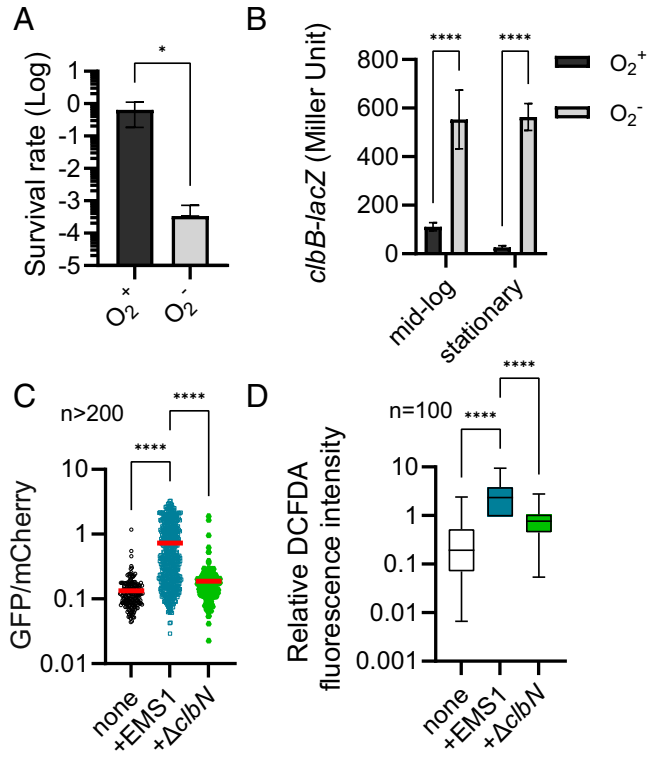

Fig. 4. Colibactin induces SOS response and ROS accumulation in *V. cholerae*. (*A*) O_2 affects EMS1 inhibition of *V. cholerae* growth. *V. cholerae* alone or cocultured with EMS1 was grown aerobically or microaerobically in M9 medium for 24 h. Viable *V. cholerae* CFU values were then determined. The mean of three independent assays is shown, and error bars represent the SD; *$P < 0.05$ (*t* test). (*B*) *clb* expression. EMS1 harboring a chromosomal *clbB–lacZ* transcriptional fusion was grown aerobically and microaerobically. At the growth phase indicated, samples were withdrawn, and β-galactosidase activity was measured. The mean of three independent assays is shown, and error bars represent the SD; ****$P < 0.0001$ (one-way ANOVA). (*C*) Induction of SOS response. *V. cholerae* harboring chromosomal P*recA-gfp* and P*tet-mCherry* reporters was inoculated alone or with either EMS1 or Δ*clbN* mutants into M9 medium. The cultures were grown for 16 h, and then green fluorescent protein (GFP) and mCherry intensity of each *V. cholerae* cell was measured using a Nikon NiU fluorescence microscope. For each condition, 200 cells were analyzed; ****$P < 0.0001$ (two-way ANOVA). (*D*) ROS accumulation staining assay of *V. cholerae* when cocultured with EMS1 and colibactin-deficient *clbN* mutant. *V. cholerae* harboring a chromosomal P*tet-mCherry* reporter was inoculated alone and with EMS1 or Δ*clbN* mutants in M9 medium. The cultures were grown for 24 h, and DCFDA staining was performed and visualized using the GFP filter and normalized against mCherry intensity. For each condition, 100 cells were analyzed; ****$P < 0.0001$ (two-way ANOVA).

have more efficient endogenous DNA repair machineries with faster induction in response to damaging stimuli. In addition, many other factors that control bacterial SOS response may also contribute to differential sensitivity toward colibactin.

Colibactin Expression and Specific Microbial Targeting Is Associated with Altered Microbiota Composition in Humans and Mice. In cholera-endemic areas, human gut microbiomes recurrently enter a dysbiotic state characterized by low microbial diversity after disruption by cholera and noncholeric diarrhea, malnutrition, and other regular environmental insults (6, 38). This has been demonstrated to be a driver of disease susceptibility through the loss of key biochemical functions, such as microbial quorum sensing and bile acid metabolism (5). Colibactin-specific effects on the gut microbiome under specific conditions have been previously reported in mice. A prior study inoculated pregnant mice with colibactin-producing or colibactin-knockout *E. coli* and evaluated the response of the gut microbiome of the resulting pups (39). Using this mother-to-pup transmission mouse model, they observed colibactin-dependent phylum-level changes and a reduction in overall abundance 35 d after birth. While this is a measure of the effect of colibactin-producing microbes on microbial succession, or the ordered colonization of microbes after birth, the microbes found within immature animals and humans can differ dramatically from those of adults (40, 41). The long time horizons of these studies, coinciding with early life development and dietary transition after weaning, may also obscure specific colibactin-dependent changes in the gut microbial community. To probe commensal–colibactin interactions that are diet and host development independent that may be relevant in human populations, we colonized streptomycin-treated mice with either EMS1 or Δ*clbN* mutant. One day before *E. coli* was inoculated, streptomycin was removed from the drinking water, and the fecal gut microbial community was monitored by 16S ribosomal RNA gene sequencing (42) (Dataset S2). We found that both EMS1 and Δ*clbN* mutants colonized the colon similarly (*SI Appendix*, Fig. S7), suggesting that colibactin is not required for EMS1 colonization in this model. In contrast to Tronnet et al. (39), we identified rapid and strong community-level differences and species-level microbial taxa in the fecal microbiome of these animals that varied strongly as a function of the presence of EMS1 versus the isogenic Δ*clbN* strain. Using principal coordinates analysis of weighted UniFrac distances between fecal microbiomes, we demonstrated that fecal microbial communities diverged strongly and significantly between mice colonized with EMS1 and Δ*clbN* 5 d postcolonization (Fig. 6*A*). At the species level, our data show a dramatic depletion of *Bacteroides fragilis* and *Enterococcus* species in mice and the simultaneous enrichment of *Aerococcus* sp., *Clostridium paraputrificum*, *Actinomycetales* sp., and *Coprococcus* sp. (Fig. 6*B* and *SI Appendix*, Fig. S8).

Since several recent studies have demonstrated that the structure of the human gut microbiome can be a driver of *V. cholerae* infection outcomes, we next aimed to describe commensal gut microbiome changes associated with microbial colibactin production. We used MetaPhlAn3 analysis, which predicts the taxonomic composition of microbiomes from the human prospective cholera cohort metagenomic data to examine taxa that exhibited differential relative abundance between *clb*$^+$ and *clb*$^-$ individuals in either SYM, ASYM, or UNI groups (*SI Appendix*, Fig. S8). In general, we observed more similar microbial abundance patterns within the ASYM and SYM groups than in the UNI population, which exhibited higher intragroup variation. Several species belonging to the genera *Corynebacterium* and *Prevotella* were more likely to coexist with the colibactin-producing strains in SYM microbiomes, but intragenus variation was observed, with *Corynebacterium afermentans* and *Prevotella disiens* exhibiting lower relative abundance in the presence in *clb*$^+$ individuals. *Treponema berlinense*, *Campylobacter jejuni*, and *Trueperella bernardiae* abundance was higher in the *clb*$^+$ subpopulation of the UNI group, while *Bifidobacterium bifidum*, *Tissierellia* bacterium KA00581, and *Mycoplasma hominis* were reduced. Species belonging to *Enterococcus* displayed decreased abundance in *clb*$^+$-infected contacts except *Enterococcus cecorum* in ASYM individuals. Among species in the genus *Bacteroides*, *Bacteroides caccae* and *Bacteroides plebeius* were higher. Strikingly, levels of *B. fragilis* were lower in *clb*$^+$ ASYM individuals, similar to in vitro and in vivo killing results in microcosms with EMS1 or *clb*$^-$ mutants (Fig. 6*C*).

We confirmed that colibactin-producing *E. coli* are able to target *B. fragilis* by repeating our in vitro assays with *B. fragilis*

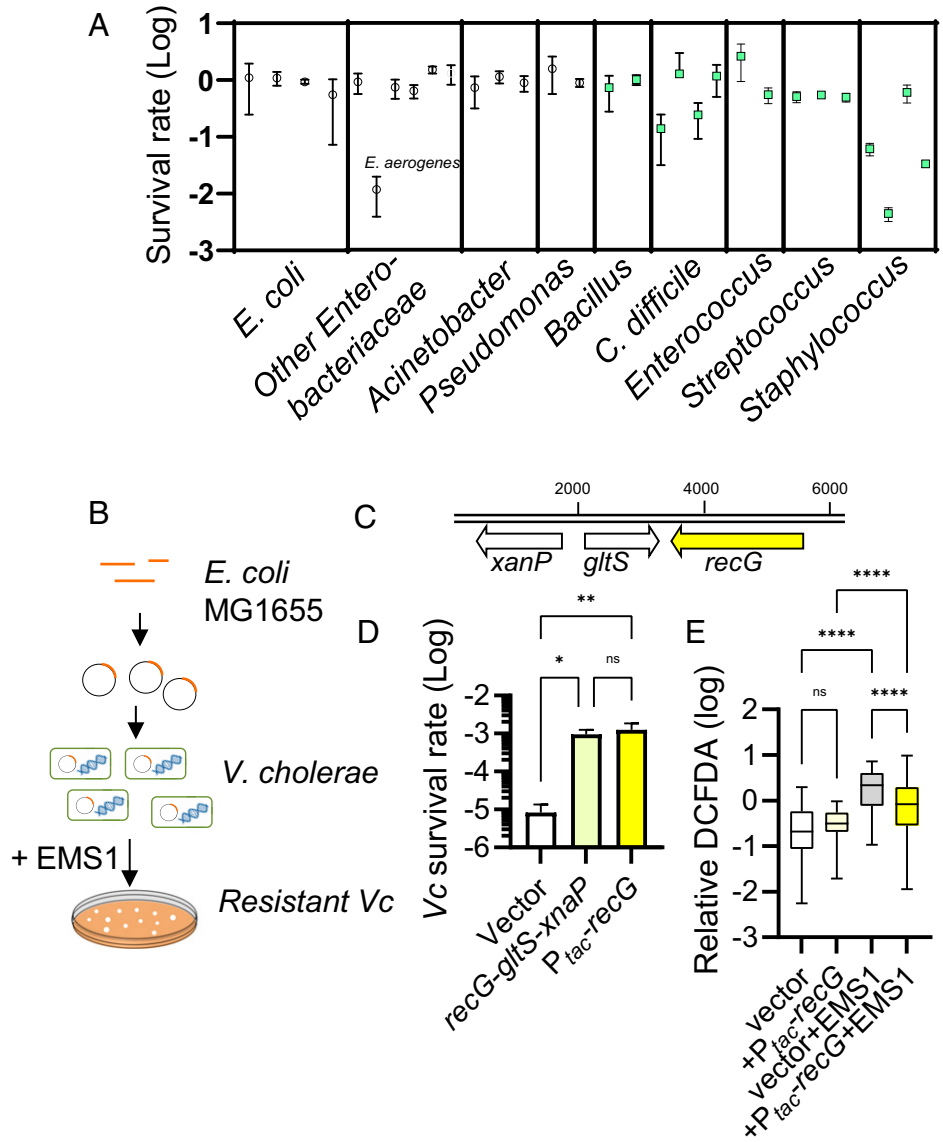

Fig. 5. The effects of colibactin on the growth of different bacterial species. (*A*) Inhibitory effects of EMS1. Approximately 10^6 CFU/mL overnight cultures of bacteria tested were inoculated into M9 plus 1% LB with 10^7 CFU/mL of either EMS1 or Δ*clbN* and incubated at 37 °C microaerobically, except *C. difficile*, which was incubated in an anaerobic chamber. After 24 h, the CFU values of assayed strains were determined, and the survival rate was calculated by dividing CFU with EMS1 by CFU with Δ*clbN*. The mean of three independent assays is shown, with error bars representing SD. (*B*) Screening scheme for the *E. coli* EMS1-resistant factors. (*C*) The genomic structure of the *recG* region in MG1655. (*D*) *E. coli* RecG confers *V. cholerae* resistance to EMS1. *V. cholerae* with an *E. coli* expression library plasmid containing a *recG* fragment or P*tac-recG* plasmid was grown with EMS1 in M9 for 24 h. CFU values of viable *V. cholerae* were determined. ns, no significance; **P* < 0.05; ***P* < 0.01 (one-way ANOVA). (*E*) Reduced ROS accumulation in *recG*-overexpressing *V. cholerae* via staining assay of *V. cholerae* when cocultured with EMS1 and colibactin-deficient *clbN* mutant. *V. cholerae* harboring chromosomal P*tet-mCherry* reporter and containing either vector or plasmid-overexpressing *recG* were inoculated alone or with EMS1 into M9 medium. The cultures were grown for 24 h, and DCFDA staining was performed and visualized using the GFP filter and normalized against mCherry intensity. For each condition, 100 cells were analyzed; *****P* < 0.0001 (two-way ANOVA).

and either EMS1 or Δ*clbN* and showed strong colibactin-driven killing of *B. fragilis* by EMS1 (Fig. 6*D*). To confirm that this interaction occurs in vivo, we cointroduced *B. fragilis* and either EMS1 or Δ*clbN* into suckling mice that had their native microflora cleared with streptomycin treatment before gavage; the presence of functional colibactin biosynthesis again corresponded to significantly reduced *B. fragilis* colonization (Fig. 6*E*). Interestingly, this effect is species specific, as in vitro assays demonstrated no colibactin-dependent killing of other *Bacteroides* species, such as *Bacteroides thetaiotaomicron* and *Bacteroides vulgatus* (Fig. 6*F*). Taken together with in vitro survival assays (Fig. 5*A*), these findings again suggest that colibactin antibacterial effects may be highly species or strain specific outside of *Vibrio*. In complex fecal communities, colibactin-driven differences in individual species abundance may also be indirectly mediated via targeting of members of microbial syntrophic relationships or overall changes in gut environmental conditions.

Further comparisons of murine and human microbiome datasets revealed additional similarities in pattern. We examined *clb*$^+$ and *clb*$^-$ humans by exposure outcome class for the abundance of species belonging to the genera *Bacteroides*, *Clostridium*, *Enterococcus*, and *Coprococcus* and order *Actinomycetales*, which showed the strongest colibactin-dependent differences in vivo in colonized mice (Fig. 6*G* and *SI Appendix*, Fig. S9). In accordance with the mouse gut microbiome findings, *B. fragilis* was significantly reduced in the *clb*$^+$ individuals in both ASYM and SYM groups. Species specificity in association with *clb* status was again observed, with *clb*$^+$ individuals showing higher relative abundance of *B. plebeius* and *B. caccae*

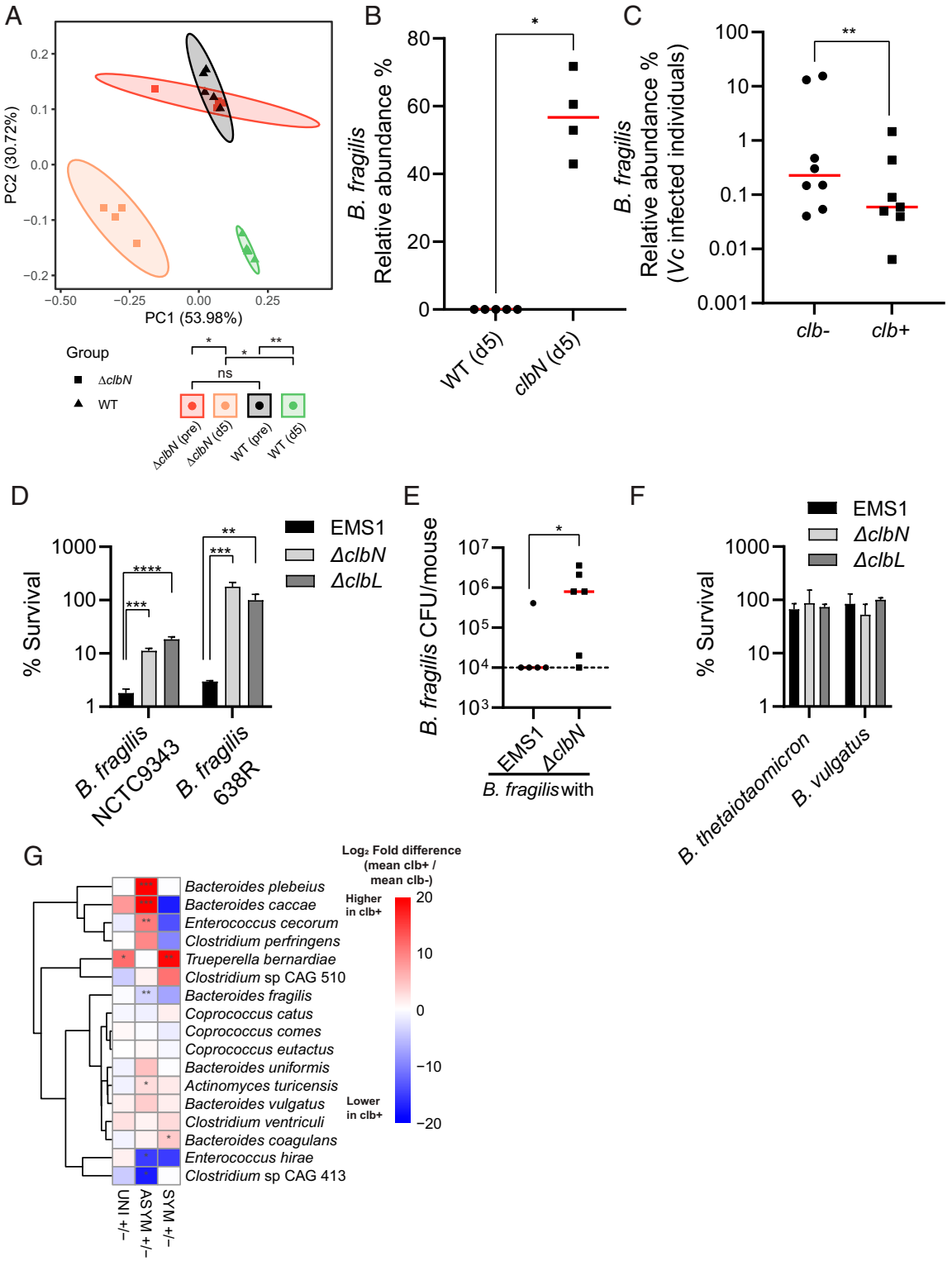

Fig. 6. Colibactin drives changes in the gut microbiome in mice and humans and specifically kills *B. fragilis*. (*A*) PCoA of mouse microbial communities from fecal samples based on weighted UniFrac distance. Ellipses show 95% confidence intervals. Statistical tests by permutational multivariate ANOVA indicate significantly different microbiome structures between the Δ*clbN* mutant and EMS1; Δ*clbN*, $n = 4$; EMS1, $n = 5$. *$P < 0.05$; **$P < 0.01$. ns, no significance. (*B*) Relative abundance of *B. fragilis* in EMS1- and Δ*clbN*-treated animals day 5 after inoculation. Mann–Whitney *U* test; *$P < 0.05$; **$P < 0.01$. (*C*) Extrapolated *B. fragilis* relative abundances by MetaPhlAn3 analysis in presymptomatic fecal samples of humans exposed to *V. cholerae* by presence of colibactin biosynthetic genes; **$P < 0.01$ edgeR. (*D*) Colibactin effects on *B. fragilis* growth in vitro. Approximately 10^6 CFU/mL overnight cultures of *B. fragilis* tested were inoculated into M9 plus 1% BHI (Brain Heart Infusion) with 10^7 CFU/mL of EMS1, Δ*clbN*, or Δ*clbL* and incubated at 37 °C anaerobically. After 24 h, CFU values of assayed strains were determined, and the survival rate was calculated by dividing CFU with *E. coli* by CFU without *E. coli*. The mean of three independent assays is shown, with error bars representing SDs; **$P < 0.01$; ***$P < 0.0005$; ****$P < 0.0001$ (one-way ANOVA). (*E*) Effects of coinoculation of EMS1 and Δ*clbN* in suckling mice. Levels of *B. fragilis* in small intestine determined by plating after 16 h of colonization. Mann–Whitney *U* test; *$P < 0.05$. (*F*) Colibactin does not kill related *Bacteroides* commensals. Commensal *Bacteroides* strains were incubated with EMS1, Δ*clbN*, or Δ*clbL* at 37 °C anaerobically. After 24 h, CFU values of assayed strains were determined, and the survival rate was calculated by dividing CFU with *E. coli* by CFU with *Bacteroides* grown alone. The mean of three independent assays is shown, with error bars representing SD. (*G*) Distribution of the species in genera exhibiting highest colibactin-dependent changes in mice from household contacts of confirmed cholera patients in Bangladesh. Species with relative abundance >1% in at least one sample across the whole dataset (Dataset S3) are shown; edgeR: *$P < 0.05$; **$P < 0.01$; ***$P < 0.001$.

in the ASYM group and *Bacteroides coagulans* in SYM individuals. *Actinomycetales*, *T. bernardiae*, and *Actinomyces turicensis* were enriched in SYM/UNI and ASYM individuals separately. *Enterococcus hirae* was observed at a lower abundance in the ASYM *clb*$^+$ population, while *E. cecorum* exhibited the opposite trend. Taken together these data demonstrate that in vitro and in vivo in humans and mice, colibactin production is associated with strong effects on gut commensal bacteria, providing direct evidence that this commensal-derived genotoxin plays a role in shaping the enteric microbiome and in modulating the infectiousness of pathogenic bacteria.

Discussion

The host gut microbiota has a significant impact on the susceptibility of hosts to infection by enteropathogens, including *V. cholerae* (43, 44). Gut commensals are known to produce antagonistic metabolites against *V. cholerae* infections. Here, we identified a *pks*$^+$ B2 family commensal *E. coli*, EMS1, from the adult mouse intestine that can antagonize *V. cholerae* growth in vitro and gut colonization in vivo. The anti-*Vibrio* activity of EMS1 depends on the production of the genotoxin colibactin. We demonstrated that EMS1 colibactin damages bacterial DNA and reshapes the host gut microbiota, thus exemplifying the multifaceted role of a commensal-produced genotoxin in contributing to the dynamics of the host gut microbiome.

Anti-*Vibrio* Commensals and Their Mechanisms of Action. Commensal microbiotas protect hosts from *V. cholerae* colonization and infection (2, 45). Studies of individual gut microbes have revealed a number of possible mechanisms contributing to colonization resistance against *V. cholerae*. *Lactobacillus* species from cholera patient fecal samples (13) or from the stool of healthy children (46) were reported to produce diffusible compounds inhibitory against *V. cholerae* or its in vitro biofilm formation and dispersal. Oral feeding of infant mice with *Lactococcus lactis* reduced *V. cholerae* growth and colonization in vivo, depending on the production of lactic acid (9). A commensal *E. coli* from a healthy human gut or probiotic *E. coli* Nissle 1917 can metabolize glucose to lower pH to kill *V. cholerae* in vitro (47) or reduce *V. cholerae* colonization in a zebrafish model (12). *V. cholerae* is sensitive to acidic pH (pH < 5), and lowering local environmental pH by gut microbes provides an effective mechanism to prevent *V. cholerae* infection. The mouse commensal EMS1 potently inhibited *V. cholerae* growth in vitro (Fig. 1) and conferred colonization resistance in vivo (Fig. 3), and it is likely to use a different antagonistic mechanism because coculture did not lower pH compared to *Vc* monoculture (*SI Appendix*, Fig. S3).

Gut commensals can also secrete small molecules to interfere with the virulence signaling of *V. cholerae*. *Blautia obeum*, a human gut commensal, provided major colonization resistance to *V. cholerae* via production of autoinducer-2 (AI-2) (6). AI-2 is a cell density–dependent signal molecule that mediates bacterial cell–cell communication; *B. obeum* AI-2 led to repression of several factors critical for *V. cholerae* colonization. You et al. (14) reported that a mouse commensal *B. vulgatus* suppresses *V. cholerae* infection in mice by competing for compounds that enhance *V. cholerae* proliferation and promoting the accumulation of compounds inhibitory toward *V. cholerae* growth, including short-chain fatty acids. Here, we found that EMS1-mediated antagonism relies on a *pks* genomic island frequently found in *E. coli* belonging to the B2 phylogroup and encoding the genotoxin colibactin. *pks*$^+$ *E. coli* have been linked to human colorectal cancer, as the secondary metabolite colibactin, functioning as a genotoxin, cross-links DNA, transforms gut epithelial cells, and contributes to tumorigenesis (15, 16). The discovery of bactericidal activity of *pks*$^+$ *E. coli* suggested that this family of bacteria may protect the host from pathogen infections as well as affect the composition of gut microbiota more generally.

***pks*$^+$ *E. coli* and Colibactin.** EMS1 was isolated from the small intestine of an adult mouse, a niche where *V. cholerae* colonization takes place. EMS1 shares extensive genomic synteny with *pks*$^+$ B2 *E. coli*, including uropathogenic *E. coli* CFT073 and the probiotic *E. coli* Nissle 1917 (*SI Appendix*, Fig. S2), both of which are *pks*$^+$ B2 *E. coli*. These *pks*$^+$ *E. coli* strains all produce colibactin and are frequently found in colon cancer patients and, to a lesser extent, in healthy individuals. EMS1 colibactin potently killed *Vibrio* spp. and moderately inhibited other pathogens, including *E. aerogenes* and a subgroup of *Staphylococcus* spp. These findings expand upon a recent report that found that colibactin exhibited modest antibiotic activity to *S. aureus* (37) and also suggest that colibactin is able to act like a bacteriocin against diverse microbial targets in the gut. In *V. cholera,* colibactin killing is cell contact dependent (Fig. 1*E* and ref. 21), and this may result from the highly unstable nature of colibactin or contact requirements for colibactin secretion or delivery. Production of colibactin in other *pks*$^+$ *E. coli* is affected by a number of genetic and environmental cues (15), including iron and carbon sources. We found that EMS1 *clbB* gene expression and colibactin killing was activated when EMS1 was grown in low-nutrient medium with glucose microaerobically (Fig. 4), but no killing effect was detected in rich LB medium or aerobically (shaking). Such differences again may reflect the unstable and contact-dependent nature of colibactin. Colibactin cross-links interstrand DNA and induces DNA DSBs due to a unique structure that has two electrophilic cyclopropane warheads at both ends (48, 49). EMS1 colibactin caused DNA damage responses in HeLa cells and in hemolymph cells of wax moth (*SI Appendix*, Fig. S5), as expected due to its known role in damaging eukaryotic DNA. EMS1 colibactin also damaged *V. cholerae* DNA, activated the SOS response, and induced intracellular ROS accumulation (Fig. 4), suggesting that a possible mechanism of colibactin-mediated bacterial killing is through DSB-caused cell death. Interestingly, many bacteria, including *E. coli*, are resistant to colibactin killing due to production of a cyclopropane hydrolase ClbS that directly inactivates colibactin (50, 51). The discovery that ectopic expression of *recG*, an *E. coli* DNA helicase gene that repairs DNA DSBs (52), can suppress ROS accumulation and protect *Vc* from killing by colibactin (Fig. 5) further supports a role for colibactin in inducing DSBs to kill bacteria. We speculate that bacteria possessing either *clbS* or a robust DNA repair system may be more resistant to *pks*$^+$ *E. coli* antagonism.

Colibactin and the Gut Microbiota. In addition to an inhibitory effect toward both *V. cholerae* and other gut-associated bacteria in vitro, EMS1 directly inhibited *V. cholerae* colonization and affected gut microbiome composition by driving lower levels of *B. fragilis* in an adult mouse model, which was confirmed in direct in vitro killing assays. These data provide direct evidence that *E. coli*–derived colibactin plays a role in shaping the enteric microbiome, thereby potentially modulating the metabolic functions of the gut commensal communities and thus interactions with invading pathogens. An analysis of the metagenomic data of household contacts of cholera patients

showed a relatively lower abundance of *pks* islands in infected SYM contacts as opposed to those infected ASYM or UNI household contacts, suggesting that the effects of colibactin may be associated with cholera outcomes in human populations. Using antibiotic-treated adult mice, we identified potential species that respond to colibactin, observing depletion especially of *B. fragilis* and *Enterococcus* sp. but enrichment of *Aerococcus* sp., *C. paraputrificum*, *Actinomycetales* sp., and *Coprococcus* sp. These findings were mirrored in the human gut microbiome data, where we found that *B. fragilis* and *E. hirae* were decreased in communities containing the *clb* cluster, results that were confirmed with *B. fragilis* using in vitro colibactin-dependent killing assays. *B. fragilis* is a common enteric commensal that is able to modulate the maturation of the immune system (53), although toxigenic strains are responsible for anaerobic infections in several body sites (54) and for infectious diarrhea in Bangladesh (55, 56). An association of *B. fragilis* with colibactin-producing *E. coli* in interspecies biofilms exists in colorectal cancer patients (57), with an interaction between colibactin$^+$ *E. coli* and toxigenic *B. fragilis* leading to modulation of tumorigenesis in susceptible animals. However, previous work has not identified a role for colibactin-driven killing of either toxigenic or commensal *B. fragilis*; no significant changes in the levels of *B. fragilis* and *pks*$^+$ *E. coli* were noted upon cocolonization. Other genotoxins have also been associated with microbiome changes in mice, including the cytolethal distending toxin (CDT) from *C. jejuni* (58). *C. jejuni* was enriched in communities containing *clb* in UNI individuals. While specific microbial CDT targeting is not described, these findings highlight the possibility of specific interactions between microbial genotoxins in modifying complex gut communities. In contrast to prior studies, we demonstrated the growth-inhibiting effects on *V. cholerae* of colibactin derived from a native mouse isolate, expanding the functional range of colibactin to include antibacterial functions in addition to activity against eukaryotes.

Serving as a disruptive and competitive factor, colibactin can affect the species composition and thus the biochemical environment of host environments encountered by pathogenic bacteria. Colibactin-dependent effects on commensal and pathogenic bacteria may work via different mechanisms, whether by direct contact- or proximity-dependent killing for *V. cholerae* or indirectly through modulation of the fitness or metabolic activities of commensals that produce necessary metabolites for other members of the community. Bactericidal function may also be modulated by other environmental factors besides proximity; in studies of colorectal cancer tissues (57), an association with *pks*$^+$ *E. coli* and enterotoxigenic *B. fragilis* was noted, although no colonization differences as a function of cocolonization were observed. Our findings also highlight the strain specificity of commensal–pathogen interactions and the limits of 16S amplicon sequencing approaches in identifying these. Previous studies showed that the presence of some murine commensal *E. coli* was able to promote virulence (59); highly strain-specific associations of *E. coli* with infection outcomes are likely in human populations, especially given that phylotype B2 group *E. coli* are variably distributed in humans (60) and that the observed intragenus variance in the ability of colibactin to kill both pathogenic and commensal gut-associated bacteria. The regulation of colibactin production by nutrient condition further complicates our understanding of how this factor integrates into interspecies dynamics in complex microbiomes; rapid changes in the nutritional environment of the gut can be driven by host diet and commensal microbial metabolism. Further experimentation will be required to elucidate the complex potential interactions between specific commensal genotoxin targets and their subsequent effects on gut microbiome structure.

Materials and Methods

Strains, Plasmids, and Culture Conditions. *V. cholerae* El Tor C6706 was used as the primary wild-type strain in this study. The *E. coli* strain EMS1 was isolated from the small intestine of a CD-1 adult mouse. Both *V. cholerae* and *E. coli* were propagated in LB Miller medium with appropriate antibiotics at 30 °C and 37 °C, respectively, unless otherwise noted. All other bacterial strains used in this study are described in *SI Appendix*, Tables S1 and S2. The detailed description of constructs of deletion strains and transcriptional reporters is provided in the *SI Appendix*, *Supplemental Methods and Materials*.

***V. cholerae* Inhibitory Assays by EMS1.** Unless otherwise indicated, 10^5 CFU/mL *V. cholerae* from overnight cultures was inoculated alone or with 10^6 CFU/mL EMS1 or EMS1-derived mutants into M9-glucose medium (10 mM HEPES, pH 7.4, was added to buffer pH). The cultures were incubated at 37 °C microaerobically (no shaking) for 24 h. Viable *V. cholerae* cells were determined by serial dilution and plating on selective LB plates (usually containing streptomycin [100 μg/mL] and polymyxin B [6 μg/mL]).

Screens of EMS1 Mutants that Lost Anti-*Vibrio* Activity. Approximately 3,000 Tn5 insertional mutants of EMS1 were inoculated into 96-well plates containing M9 medium with C6706 (pBAD-lux) and incubated at 37 °C for 24 h. LB medium containing 0.1% arabinose (to induce P_{BAD}-lux) and streptomycin (to inhibit EMS1 growth) was added, and the plates were incubated at 37 °C with shaking for 2 h. Luminescence was then measured. Transposon mutants that were unable to inhibit *V. cholerae* growth, as identified by high luminescence wells, were then purified, and transposon insertion was determined using arbitrary PCR (61) and sequencing.

Identification of Colibactin-Resistant Factors. The *E. coli* MG1655 genomic library plasmids were introduced into *V. cholerae* by conjugal transfer. The *V. cholerae* library was then incubated with EMS1 (pMal-c2x) in M9 medium microaerobically for 24 h at 37 °C. The recovered *V. cholerae* cells were incubated with EMS1 for another round of selection. The resistant *V. cholerae* isolates were purified, and the plasmid was extracted for sequencing analysis.

Human Metagenomic Data Analysis. The Bangladesh human metagenomic data were obtained from Levade et al. (62), accession number PRJNA608678. The results from a total of 82 individuals, for individuals that had multi–time point samples, were summed up. To test the presence of *clb*, the human metagenomic reads were aligned to the *clb* cluster (*clbA-S*) using blastn, with the E value cutoff of 0.00001. MetaPhlAn3 (63) was then used to profile the composition of the gut microbial community of each individual at day 2. To obtain species that might respond to colibactin, edgeR (64) was used to calculate the fold change and significance of intergroup differences. Species reaching a maximum relative abundance of at least 1% in at least one sample were retained for further analysis.

Data Availability. The complete genome sequence of *E. coli* EMS1 is deposited in the National Center for Biotechnology Information (NCBI) GenBank (accession no. CP072942). The 16S sequence data have been deposited in NCBI under BioProject number PRJNA768438. All other study data are included in the article and/or supporting information.

ACKNOWLEDGMENTS. We thank Drs. Anna Cobian Guemes, Frederick Bushman, Zane Liu, and Jessie Larios Valencia for helpful discussions and technical support. We would also like to thank Dr. Joseph Zackular for providing many strains used in the study. This study is supported by NIH Grants AI137283, AI120489 (J.Z.), AI157106 (J.Z., A.H.), GM124724 (A.H.), and GM080279 (M.G.).

Author affiliations: [a]Department of Microbiology, University of Pennsylvania Perelman School of Medicine, Philadelphia, PA 19104; [b]Department of Microbiology & Plant Pathology, University of California, Riverside, CA 92521; [c]Harriton High School, Bryn Mawr, PA 19010; [d]Department of Microbiology and Immunology, Drexel University College of Medicine, Philadelphia, PA 19102; and [e]Department of Biology, University of Pennsylvania, Philadelphia, PA 19104

1. I. Sekirov, S. L. Russell, L. C. Antunes, B. B. Finlay, Gut microbiota in health and disease. *Physiol. Rev.* **90**, 859–904 (2010).
2. R. Freter, Experimental enteric *Shigella* and *Vibrio* infections in mice and guinea pigs. *J. Exp. Med.* **104**, 411–418 (1956).
3. L. García-Bayona, L. E. Comstock, Bacterial antagonism in host-associated microbial communities. *Science* **361**, eaat2456 (2018).
4. T. D. Lawley, A. W. Walker, Intestinal colonization resistance. *Immunology* **138**, 1–11 (2013).
5. S. Alavi *et al.*, Interpersonal gut microbiome variation drives susceptibility and resistance to cholera infection. *Cell* **181**, 1533–1546 (2020).
6. A. Hsiao *et al.*, Members of the human gut microbiota involved in recovery from *Vibrio cholerae* infection. *Nature* **515**, 423–426 (2014).
7. S. B. Peterson, S. K. Bertolli, J. D. Mougous, The central role of interbacterial antagonism in bacterial life. *Curr. Biol.* **30**, R1203–R1214 (2020).
8. J. Zhu *et al.*, Quorum-sensing regulators control virulence gene expression in *Vibrio cholerae*. *Proc. Natl. Acad. Sci. U.S.A.* **99**, 3129–3134 (2002).
9. N. Mao, A. Cubillos-Ruiz, D. E. Cameron, J. J. Collins, Probiotic strains detect and suppress cholera in mice. *Sci. Transl. Med.* **10**, eaao2586 (2018).
10. F. Duan, J. C. March, Engineered bacterial communication prevents *Vibrio cholerae* virulence in an infant mouse model. *Proc. Natl. Acad. Sci. U.S.A.* **107**, 11260–11264 (2010).
11. A. Focareta, J. C. Paton, R. Morona, J. Cook, A. W. Paton, A recombinant probiotic for treatment and prevention of cholera. *Gastroenterology* **130**, 1688–1695 (2006).
12. D. Nag, P. Breen, S. Raychaudhuri, J. H. Withey, Glucose metabolism by *Escherichia coli* inhibits *Vibrio cholerae* intestinal colonization of zebrafish. *Infect. Immun.* **86**, e00486-18 (2018).
13. S. H. Silva, E. C. Vieira, R. S. Dias, J. R. Nicoli, Antagonism against *Vibrio cholerae* by diffusible substances produced by bacterial components of the human faecal microbiota. *J. Med. Microbiol.* **50**, 161–164 (2001).
14. J. S. You *et al.*, Commensal-derived metabolites govern *Vibrio cholerae* pathogenesis in host intestine. *Microbiome* **7**, 132 (2019).
15. M. W. Dougherty, C. Jobin, Shining a light on colibactin biology. *Toxins (Basel)* **13**, 346 (2021).
16. T. Faïs, J. Delmas, N. Barnich, R. Bonnet, G. Dalmasso, Colibactin: More than a new bacterial toxin. *Toxins (Basel)* **10**, E151 (2018).
17. T. M. Wassenaar, *E. coli* and colorectal cancer: A complex relationship that deserves a critical mindset. *Crit. Rev. Microbiol.* **44**, 619–632 (2018).
18. M. Lasaro *et al.*, *Escherichia coli* isolate for studying colonization of the mouse intestine and its application to two-component signaling knockouts. *J. Bacteriol.* **196**, 1723–1732 (2014).
19. J. Zhu *et al.*, Data from: Escherichia coli strain EMS1 chromosome. National Center for Biotechnology Information. https://www.ncbi.nlm.nih.gov/nuccore/CP072942. Deposited 26 August 2021.
20. J. Reidl, K. E. Klose, *Vibrio cholerae* and cholera: Out of the water and into the host. *FEMS Microbiol. Rev.* **26**, 125–139 (2002).
21. J. P. Nougayrède *et al.*, *Escherichia coli* induces DNA double-strand breaks in eukaryotic cells. *Science* **313**, 848–851 (2006).
22. C. A. Brotherton, E. P. Balskus, A prodrug resistance mechanism is involved in colibactin biosynthesis and cytotoxicity. *J. Am. Chem. Soc.* **135**, 3359–3362 (2013).
23. Y. Jiang *et al.*, Reactivity of an unusual amidase may explain colibactin's DNA cross-linking activity. *J. Am. Chem. Soc.* **141**, 11489–11496 (2019).
24. M. Xue *et al.*, Structure elucidation of colibactin and its DNA cross-links. *Science* **365**, eaax2685 (2019).
25. X. Bian *et al.*, In vivo evidence for a prodrug activation mechanism during colibactin maturation. *ChemBioChem* **14**, 1194–1197 (2013).
26. X. Bian, A. Plaza, Y. Zhang, R. Müller, Two more pieces of the colibactin genotoxin puzzle from *Escherichia coli* show incorporation of an unusual 1-aminocyclopropanecarboxylic acid moiety. *Chem. Sci. (Camb.)* **6**, 3154–3160 (2015).
27. M. I. Vizcaino, P. Engel, E. Trautman, J. M. Crawford, Comparative metabolomics and structural characterizations illuminate colibactin pathway-dependent small molecules. *J. Am. Chem. Soc.* **136**, 9244–9247 (2014).
28. Z. R. Li *et al.*, Critical intermediates reveal new biosynthetic events in the enigmatic colibactin pathway. *ChemBioChem* **16**, 1715–1719 (2015).
29. T. Pérez-Berezo *et al.*, Identification of an analgesic lipopeptide produced by the probiotic *Escherichia coli* strain Nissle 1917. *Nat. Commun.* **8**, 1314 (2017).
30. C. S. Kim, T. Turocy, G. Moon, E. E. Shine, J. M. Crawford, *Escherichia coli*-derived γ-lactams and structurally related metabolites are produced at the intersection of colibactin and fatty acid biosynthesis. *Org. Lett.* **23**, 6895–6899 (2021).
31. G. Cuevas-Ramos *et al.*, *Escherichia coli* induces DNA damage in vivo and triggers genomic instability in mammalian cells. *Proc. Natl. Acad. Sci. U.S.A.* **107**, 11537–11542 (2010).
32. C. R. Lammert *et al.*, AIM2 inflammasome surveillance of DNA damage shapes neurodevelopment. *Nature* **580**, 647–652 (2020).
33. K. Drlica, X. Zhao, DNA gyrase, topoisomerase IV, and the 4-quinolones. *Microbiol. Mol. Biol. Rev.* **61**, 377–392 (1997).
34. M. A. Kohanski, D. J. Dwyer, B. Hayete, C. A. Lawrence, J. J. Collins, A common mechanism of cellular death induced by bactericidal antibiotics. *Cell* **130**, 797–810 (2007).
35. Y. Liu, J. A. Imlay, Cell death from antibiotics without the involvement of reactive oxygen species. *Science* **339**, 1210–1213 (2013).
36. I. Keren, Y. Wu, J. Inocencio, L. R. Mulcahy, K. Lewis, Killing by bactericidal antibiotics does not depend on reactive oxygen species. *Science* **339**, 1213–1216 (2013).
37. T. Faïs *et al.*, Antibiotic activity of *Escherichia coli* against multiresistant *Staphylococcus aureus*. *Antimicrob. Agents Chemother.* **60**, 6986–6988 (2016).
38. L. A. David *et al.*, Gut microbial succession follows acute secretory diarrhea in humans. *mBio* **6**, e00381-15 (2015).
39. S. Tronnet *et al.*, The genotoxin colibactin shapes gut microbiota in mice. *mSphere* **5**, e00589-20 (2020).
40. J. E. Koenig *et al.*, Succession of microbial consortia in the developing infant gut microbiome. *Proc. Natl. Acad. Sci. U.S.A.* **108**, 4578–4585 (2011).
41. J. Wang *et al.*, Core gut bacteria analysis of healthy mice. *Front. Microbiol.* **10**, 887 (2019).
42. A. Hsiao *et al.*, Data from: Colibactin modulating gut microbiome. National Center for Biotechnology Information. https://www.ncbi.nlm.nih.gov/bioproject/?term=PRJNA768438. Deposited 4 October 2021.
43. J. Y. Cho, R. Liu, J. C. Macbeth, A. Hsiao, The interface of *Vibrio cholerae* and the gut microbiome. *Gut Microbes* **13**, 1937015 (2021).
44. Z. Qin, X. Yang, G. Chen, C. Park, Z. Liu, Crosstalks between gut microbiota and *Vibrio cholerae*. *Front. Cell. Infect. Microbiol.* **10**, 582554 (2020).
45. R. Freter, The fatal enteric cholera infection in the guinea pig, achieved by inhibition of normal enteric flora. *J. Infect. Dis.* **97**, 57–65 (1955).
46. S. Kaur, P. Sharma, N. Kalia, J. Singh, S. Kaur, Anti-biofilm properties of the fecal probiotic *Lactobacilli* against *Vibrio* spp. *Front. Cell. Infect. Microbiol.* **8**, 120 (2018).
47. C. Sengupta *et al.*, Cross feeding of glucose metabolism byproducts of *Escherichia coli* human gut isolates and probiotic strains affect survival of *Vibrio cholerae*. *Gut Pathog.* **9**, 3 (2017).
48. N. Bossuet-Greif *et al.*, The colibactin genotoxin generates DNA interstrand cross-links in infected cells. *mBio* **9**, e02393-17 (2018).
49. M. I. Vizcaino, J. M. Crawford, The colibactin warhead crosslinks DNA. *Nat. Chem.* **7**, 411–417 (2015).
50. P. Tripathi *et al.*, ClbS is a cyclopropane hydrolase that confers colibactin resistance. *J. Am. Chem. Soc.* **139**, 17719–17722 (2017).
51. N. Bossuet-Greif *et al.*, *Escherichia coli* ClbS is a colibactin resistance protein. *Mol. Microbiol.* **99**, 897–908 (2016).
52. B. Azeroglu *et al.*, RecG directs DNA synthesis during double-strand break repair. *PLoS Genet.* **12**, e1005799 (2016).
53. E. B. Troy, D. L. Kasper, Beneficial effects of *Bacteroides fragilis* polysaccharides on the immune system. *Front. Biosci.* **15**, 25–34 (2010).
54. H. M. Wexler, *Bacteroides*: The good, the bad, and the nitty-gritty. *Clin. Microbiol. Rev.* **20**, 593–621 (2007).
55. P. Pathela *et al.*, Enterotoxigenic *Bacteroides fragilis*-associated diarrhea in children 0-2 years of age in rural Bangladesh. *J. Infect. Dis.* **191**, 1245–1252 (2005).
56. C. L. Sears *et al.*, Association of enterotoxigenic *Bacteroides fragilis* infection with inflammatory diarrhea. *Clin. Infect. Dis.* **47**, 797–803 (2008).
57. C. M. Dejea *et al.*, Patients with familial adenomatous polyposis harbor colonic biofilms containing tumorigenic bacteria. *Science* **359**, 592–597 (2018).
58. Z. He *et al.*, *Campylobacter jejuni* promotes colorectal tumorigenesis through the action of cytolethal distending toxin. *Gut* **68**, 289–300 (2019).
59. W. Zhao, F. Caro, W. Robins, J. J. Mekalanos, Antagonism toward the intestinal microbiota and its effect on *Vibrio cholerae* virulence. *Science* **359**, 210–213 (2018).
60. J. N. V. Martinson, S. T. Walk, *Escherichia coli* residency in the gut of healthy human adults. *Ecosal Plus* **9**, 10.1128/ecosalplus.ESP-0003-2020 (2020).
61. N. Judson, J. J. Mekalanos, Transposon-based approaches to identify essential bacterial genes. *Trends Microbiol.* **8**, 521–526 (2000).
62. I. Levade *et al.*, Predicting *Vibrio cholerae* infection and disease severity using metagenomics in a prospective cohort study. *J. Infect. Dis.* **223**, 342–351 (2021).
63. F. Beghini *et al.*, Integrating taxonomic, functional, and strain-level profiling of diverse microbial communities with bioBakery 3. *eLife* **10**, e65088 (2021).
64. M. D. Robinson, D. J. McCarthy, G. K. Smyth, edgeR: A Bioconductor package for differential expression analysis of digital gene expression data. *Bioinformatics* **26**, 139–140 (2010).
65. M. J. Sullivan, N. K. Petty, S. A. Beatson, Easyfig: A genome comparison visualizer. *Bioinformatics* **27**, 1009–1010 (2011).